Protonation of Gaseous Halogenated Phenols and Anisoles and Its Interpretation Using DFT-Based Local Reactivity Indices

Oksana Tishchenko,[†] Nguyen-Nguyen Pham-Tran,[†,‡] Eugene S. Kryachko,[†,§] and Minh Tho Nguyen*[,†]

Department of Chemistry, University of Leuven, Celestijnenlaan 200F, B-3001 Leuven, Belgium, Faculty of Chemistry, College of Sciences, Vietnam National University, HoChiMinh City, Vietnam, and Bogoliubov Institute for Theoretical Physics, Kiev, Ukraine 03143

Received: March 19, 2001; In Final Form: July 2, 2001

The local proton affinities of phenol and its halogenated derivatives, $X-C_6H_4-OH$ (X = H, F, Cl, Br, and I) in the C_2 (ortho), C_3 (meta), and C_4 (para) ring carbon positions are determined using DFT and MO methods. Similar to the process in the parent phenol, the C_4-protonation is the most preferable following a X-substitution at either the C_2 or C_3 position. Except for X = I, in *para*-X-phenols, a C_2-protonation provides the most stable protonated forms; for *para*-I-phenol, a C_4-protonation remains more favorable. At the modest B3LYP/6-31+G(d,p) + ZPE level, the proton affinities (PA's) are reasonably reproduced with a quasi systematic overestimation of about 10 kJ/mol with respect to available experimental data. The calculated PA's for X-phenols are as follows (values in kJ/mol, 2, 3, and 4 stand for the substitution positions and experimental values are given in parentheses): 2-F, 797 (788); 3-F, 813 (802); 4-F, 787 (776); 2-Cl, 801; 3-Cl, 815; 4-Cl, 789; 2-Br, 806; 3-Br, 818; 4-Br, 792; 2-I, 813; 3-I, 823; and 4-I, 816; with a probable error of ± 12 kJ/mol. A portion of the potential energy surface describing the excess proton migration over the phenol ring is elaborated. A correlation between the local PA's and the shifts of the ν_{OH} and τ_{OH} vibrational modes under protonation suggests that a resonance mechanism is likely responsible for the trend of changes in PA. Attempts to rationalize the regioselectivity of protonation are made using local reactivity indices derived from density functional theory, such as the condensed Fukui function (*f*) and local softness (*s*). While these indices could predict the preferential protonation site among C(H) atoms at various positions, which are the sites of a similar nature, they are unable to differentiate either a C- or an O-protonation or even the processes at C(H) and C(X) atoms. Proton affinities of anisole ($C_6H_5-O-CH_3$) and fluoroanisoles are also evaluated (kJ/mol): anisole, 845; 2-F, 820 (exptl, 807); 3-F, 835 (826); and 4-F, 809 (796).

1. Introduction

Protonation is a simple but important chemical act. The resulting protonated form is often a pivotal intermediate that guides the subsequent steps of a chemical transformation. In a molecular system having several basic sites, the protonation turns out to be usually regioselective yielding predominantly one protonated species. Therefore, knowledge on the preferable protonation site of a polyfunctional compound is of fundamental interest in the study of chemical reactivity. The attachment of proton to a molecule A is quantified by its proton affinity, PA(A),[1] which is defined as the negative enthalpy of the reaction: $A + H^+ \rightarrow AH^+$. Although the PA of a functional group is strongly influenced by the presence of substituents, it is more or less characteristic and a comparison of their values could already allow the most favored protonation site to be determined.

Let us consider the case of phenol, C_6H_5-OH, which contains both phenyl and hydroxyl functional groups. While the PA of the phenyl moiety could be estimated from that of benzene, the PA of water provides an estimate for the PA of hydroxyl. The experimental[2] PA(H_2O) is well established at 697 ± 4 kJ/mol and supported by the most accurate theoretical estimation to date of 691 ± 1 kJ/mol, performed at the CCSD(T)/aug-cc-pV5Z level.[3] The PA of benzene[4,5] is experimentally evaluated as equal to 753 kJ/mol, although its earlier experimental values[6] range from 748 to 766 kJ/mol. In other words, in comparing the experimental values, the PA(C_6H_6) exceeds the PA(H_2O) by as much as 56 kJ/mol. Such a difference suggests that the preferential protonation of phenol should occur on the ring moiety. This is, however, not a general rule (see, e.g., ref 7). In reality, the experimental PA(phenol) of 816−818 kJ/mol, as determined by either pulsed ion cyclotron resonance equilibrium experiments[8] or high-pressure mass spectrometry[9] (for a recent review see ref 10), turns out to be substantially larger than those mentioned above, implying that the OH-group of phenol strongly influences the protonation site on the phenyl moiety. In fact, it has experimentally been demonstrated that the phenol protonation occurs well on the ring, and the phenol oxygen PA is about 55−84 kJ/mol less than the enthalpy of this reaction on phenyl group.[11] These findings were subsequently supported by ab initio MO calculations performed at the MP2/6-31G(d,p) level.[12] However, the mechanism of such protonation still remains an open question. As a matter of fact, the presence of a hydroxyl group induces four different positions on the ring susceptible for an electrophilic attack, namely, the ipso-, ortho-,

* To whom correspondence should be addressed. Fax: 32-16-327992. E-mail: minh.nguyen@chem.kuleuven.ac.be.
[†] Department of Chemistry.
[‡] Faculty of Chemistry.
[§] Bogoliubov Institute for Theoretical Physics.

10.1021/jp011017m CCC: $20.00
Published on Web 09/01/2001

SCHEME 1: Numbering of Atoms in X-Phenols (X = H, F, Cl, Br, I)

meta-, and para-carbons, relative to the hydroxyl position. One of these carbon centers will show the largest attraction for the proton, and it is legitimate to pose the question as to whether the observed regioselectivity could be rationalized and/or predicted solely on the basis of the molecular properties of the neutral substrate.

The problem of protonation sites in polyfunctional molecules is indeed the subject of a long-standing theoretical interest. The main theoretical approach for its rationalization was to design a way of partitioning the molecular charge distribution into atomic properties that show a good co-relation with PA.[13−15] The components of wave functions[16,17] constructed by multiconfigurational or spin-coupled methods has been also put forward. However, these approaches are either not quite successful or could not be extended to a larger sample of compounds. Recently, there have been attempts in using DFT-based reactivity descriptors, in both global and local senses, for the interpretation of protonation sites.[18−21] Simply put, it is a different way of decomposing a molecular electronic distribution into global and/or local indices coupled with an account for the frontier orbitals. The indices are well-defined within the framework of density functional theory. Thus, starting from the electronegativity equalization principle,[18] the global descriptors such as "group hardness" and "group electronegativity", have been defined[18] and correlated with PA of amino acids. It appears that the group hardness is more useful than the group electronegativity. More recently, the more local descriptors including the Fukui function, local atomic softness or even orbital softness, have been employed in order to interpret the protonation site in aniline.[20,21] Nevertheless, the reported results are rather perplexing. While Roy et al.[20] stated that the DFT-based local softnesses can reproduce the experimentally observed preferable protonation site, Russo et al.[21] found that the orbital Fukui indices (proportional to local softnesses) do not resolve unequivocally the dilemma of protonation sites. The latter authors[21] found in addition that the absolute hardness values of protonated anilines do not follow the maximum hardness principle. Nevertheless, a closer look at the results emphasizes that aniline perhaps does not present a favorable case for applying the indices because the identity of its protonation site is strongly dependent on the quantum chemical method employed; indeed, it switches between the nitrogen and para-carbon atoms. In this context, it would be desirable to have another look at the subject by considering the analogous phenol system which, as stated above, has a clear preference for the ring protonation. Recently, we have extensively examined the validity and limitations of these indices in interpreting the regioselectivity of a number of reactions including the radical additions,[22] nucleophilic additions,[23−25] [2+1] cycloadditions,[26,27] [2+2] cycloadditions,[28] and 1,3-dipolar cycloadditions.[29−34]

Thus, we have theoretically determined the PA's and thereby the protonation sites in the parent phenol and a series of monohalogenated phenols ($X-C_6H_5-OH$, with X = H, F, Cl, Br, and I) where X successively occupies the ortho (C_2), meta (C_3), and para (C_4) positions (Scheme 1). For a further control, calculations on the fluoroanisoles, $F-C_6H_4-O-CH_3$, whose experimental values are available, were also carried out. In a subsequent step, we have obtained the Fukui functions and local softnesses of the neutral phenols and attempted to correlate them with the protonation patterns unravelled from quantum chemical calculations.

2. Computational Methods

All ab initio molecular orbital and density functional theory calculations were carried out using the Gaussian 98 suite of programs.[35] Geometries of halophenols were optimized using the B3LYP density functional[36] and the 6-31+G(d,p) basis set. For iodine, the effective core potential (ECP)[37a] with comparable quality was employed. Vibrational frequencies were computed within the harmonic approximations. Temperature effect was neglected. For the parent phenol, additional MO calculations using the larger 6-311++G(d,p) basis set and coupled-cluster method including all singles and doubles plus perturbative corrections for the triples (CCSD(T))[42] were also considered for the sake of calibration.

There are different approaches of evaluating the global softnesses and thereby the Fukui indices.[43] Here we have adopted an approach in which the vertical ionization energies (IE) and electron affinities (EA) required to obtain global softnesses, were computed as accurate as possible.[43a] We have thus computed the vertical IEs and EAs by performing single point electronic energy calculations at the neutral optimized geometries using the B3LYP functionals in conjunction with the larger correlation consistent cc-pVDZ and cc-pVTZ[37b] basis sets. Concerning the atomic charges, the values derived from the electrostatic potentials have been chosen. This approach and basis sets were previously tested to provide consistent charges and Fukui indices, and for these properties, additional diffuse functions (such as in the aug-cc-pVTZ) do not modify the overall patterns.[43a] Throughout this paper, proton affinities are given in kJ/mol, frequencies in cm^{-1}, electron affinities, and ionization energies, unless otherwise noted, in eV.

3. Results and Discussion

A. Proton Affinities of Phenol. For the sake of simplicity, the terms "para-protonation", "meta-protonation", and "ortho-protonation" stand hereafter for a protonation occurred at the C_4, C_3, and C_2 carbon atoms of the phenyl ring, respectively. As is well-known, the parent phenol **1** favors a para-protonation.[9−12] Present calculations concur with this finding. Interestingly, the para-protonated phenol can be viewed as the lowest energy protonated form of the keto form **2** of phenol which, on the other hand, can be also considered as a para-protonated phenoxyl anion.

Notice that the keto form **2** lies 69 kJ/mol above **1** at the B3LYP/6-31+G(d,p)+ZPE level which is consistent with 71 kJ/mol derived from MP2/6-31G(d)//HF/6−31(d) calculations.[44a] Here the favor of the enol form of phenol is explained in terms of the "greater resonance energy" of the enol form **1** which is by about 126 kJ/mol (30 kcal/mol) larger than that of the keto form **2**.[44b,c] On the other hand, the sum of the bond energies of the keto form is about 59 kJ/mol (14 kcal/mol) greater than that of the enol one. Therefore, the enol form is about 126−59 = 67 kJ/mol (16 kcal/mol) more stable than the keto form!

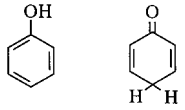

1 **2**

Upon protonation, both forms lead to the para-protonated phenol as the lowest energy structure. Table 1 compares the PA of

TABLE 1: Calculated PA's of Phenol at the para-C_4 Site

method	PA, kJ/mol
B3LYP/6-31+G(d,p)	824
B3LYP/6-311++G(d,p)[a]	820
CCSD(T)/6-31G(d,p)[b]	845
CCSD(T)/6-311++G(d,p)[b]	819
MP2/6-311++G(d,p)[b]	790
MP2/6-311++G(3df,2p)[b]	780
experiment[c]	816−818

[a] ZPE at the B3LYP/6-31G(d,p) level. [b] B3LYP/6-31G(d,p) geometries and ZPE. [c] References 8−10.

TABLE 2: Local PA's of Phenol at Different Sites

protonation site	para	ortho	meta	ipso	oxygen
PA[a]	824	814	765	706	743
PA[b]	820	809	757	699	743
PA[c]	818	808	753	679	764

[a] B3LYP/6-31+G(d,p) + ZPE, present work. [b] B3LYP/6-311++G(d,p) + ZPE, present work. [c] MP2(fc)/6−31(d,p)//HF/6-31G(d) + ZPE, ref 12.

phenol at its para-C_4 site evaluated at different theoretical levels. The CCSD(T)/6-31G(d,p) approach gives rise to a value of 845 kJ/mol which exceeds by 27 kJ/mol the upper boundary of the experimental PA. Extension of the basis set to 6-311++G(d,p) substantially improves the calculated PA by the coupled-cluster method. This indicates again the crucial role of diffuse functions in atomic basis sets in the accurate description of PA. Surprisingly, this basis and even a larger 6-311++G(3df,2p) one, within the framework of the second-order Møller−Plesset (MP2(fc)) theory (fc = frozen core approximation), result in too low PA, namely, 790 and 780 kJ/mol, respectively. Similar result was obtained within the MP2(fc)/6-311G(d)//HF/6-31G(d) approach in ref 12. The B3LYP method with moderate basis sets provides a quite satisfactory PA within limits of experimental accuracy.

We also note that, again, the B3LYP functional in conjunction with the 6-31+G(d,p) basis set provides quite accurate molecular structure and the normal vibrations for the neutral phenol molecule. Particularly, the calculated bond lengths are slightly overestimated, viz., the C−H one by about 0.3−1%, the C−C by about 0.1%, the O−H by 0.1%, and the C−O by 0.8% as compared to the experimental counterparts.[38] The predicted vibrational frequencies are comparable with the experimental values as follows: ν_{OH} = 3831 cm^{-1} (exptl = 3656 cm^{-1}),[39] τ_{OH} = 330 cm^{-1} (exptl 309 cm^{-1}),[39] and 13 (ν_{CO}) = 1284 cm^{-1} (exptl = 1261 cm^{-1})[40a,b] (in Varsányi nomenclature[41]). The normal modes 8b and 8a associated with the C=C aromatic stretching vibrations are centered at 1644 and 1654 cm^{-1} that are about 40 cm^{-1} too high with respect to the experimental ones[40a] equal to 1604 and 1609 cm^{-1}, respectively. The frequencies of the C−H *in*-plane bending vibrations (modes 18a, 18b, 9b, 9a, and 3) are overestimated by about 2%, except for the mode 3 (1360 cm^{-1}) which nearly coincides with the experimental value[40a] of 1361 cm^{-1}. Overall, it seems that the zero-point vibrational energies (ZPE) evaluated at the B3LYP/6-31+G(d,p) level are well reproduced and could be used without scaling down.

In Table 2, we gather the calculated local PA's of phenol at its different protonation sites. For the purpose of comparison, the previous results obtained at the MP2(fc)/6-31G(d,p)//HF/6-31G(d)+ZPE[12] computational level are also given. We note that an extension of the atomic basis set from 6-31+G(d,p) to 6-311++G(d,p) results in an improvement of 4−8 kJ/mol on the PA's of the phenol ring (Tables 1 and 2). All methods agree with each other in predicting the para-position as the most favorable protonation site followed by the ortho with a rather small difference of ca. 10 kJ/mol. The meta-protonated phenol is placed by ca. 59−65 kJ/mol above the para-counterpart, whereas the ipso-protonated one lies consistently much higher in energy. The difference of the PA's of both meta-C_3- and O-protonated forms ranges from 11 to 22 kJ/mol, although, in contrast to the previous results, the O-protonated form is less stable than the meta counterpart.

In summary, the potential energy surface (PES) of the protonated phenol possesses seven energy minima. They are all displayed in Figure 1 showing the portion of the B3LYP/6-31+G(d,p) PES which vividly illustrates the migration of the excess proton between the adjacent heavy atoms. This portion also includes four transition structures (TS). Starting from the highest energy ipso-protonated form, the excess H^+ almost freely migrates to the ortho-protonated one passing through a small barrier of 8 kJ/mol described by TS_3. The barriers for proton migration between the other adjacent carbon atoms are substantially larger, viz., 31 kJ/mol for the meta-to-para (TS_1) and 45 kJ/mol for the meta-to-ortho migration (TS_2). The activation barrier governing the ipso-to-oxygen migration amounts to 121 kJ/mol (TS_4). The corresponding transition frequencies of 773i, 869i, 960i, and 1599i cm^{-1}, respectively, are assigned to the vibrational modes of the excess proton parallel to the phenol ring. A large energy separation between the para-C_4 and O-protonations clearly demonstrated in Figure 1 constitutes a key difference from the analogous process of protonation in aniline ($C_6H_5-NH_2$) where both the para-C_4- and N-protonations have comparable energetics.[20−21]

The regioselectivity of the process of protonation of phenol can be easily explained in terms of its resonance structures. Drawing them, we may figure out that a positive π-charge of the protonated form is mainly localized in para- and ortho-positions with respect to the protonation site. If the OH group is attached to one of these positions, the relevant molecule is then described by four resonance structures, resulting in the positive π-charge to be distributed over all atoms. Otherwise, only three structures are allowed. A presence of a positive charge in the direct conjugation with the oxygen atom favors the electron density shift from its lone pair to the ring and strengthens a stabilization of the arenium ion. Spectroscopically, it manifests in a blue-shifting $\Delta\nu_{CO}$ of the fundamental mode 13 with the dominant contribution of the ν_{CO} stretching vibration which accompanies a shortening of the CO bond (Δr). In particular, the calculated Δr and $\Delta\nu_{CO}$ take the following values: 0.06 Å and 112 cm^{-1} in para-, 0.06 Å and 46 cm^{-1} in ortho-, and 0.03 Å, and 27 cm^{-1} in meta-protonated phenol. The other indicative frequency shifts showing the contribution of the resonance structures with the doubly bonded oxygen atom, viz.,

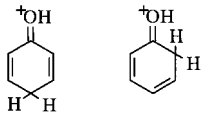

are associated with the OH stretching and torsional vibrations. The contribution of these structures is expected to weaken the OH bond and shift the corresponding ν_{OH} mode to lower frequencies. Also, it likely determines the torsional barrier describing the rotation of the OH group around the single conjugated CO bond,[45,46] and therefore, increases the τ_{OH} frequency. The low energy para-and ortho-protonated structures reveal the most pronounced and rather similar red-shifts of the

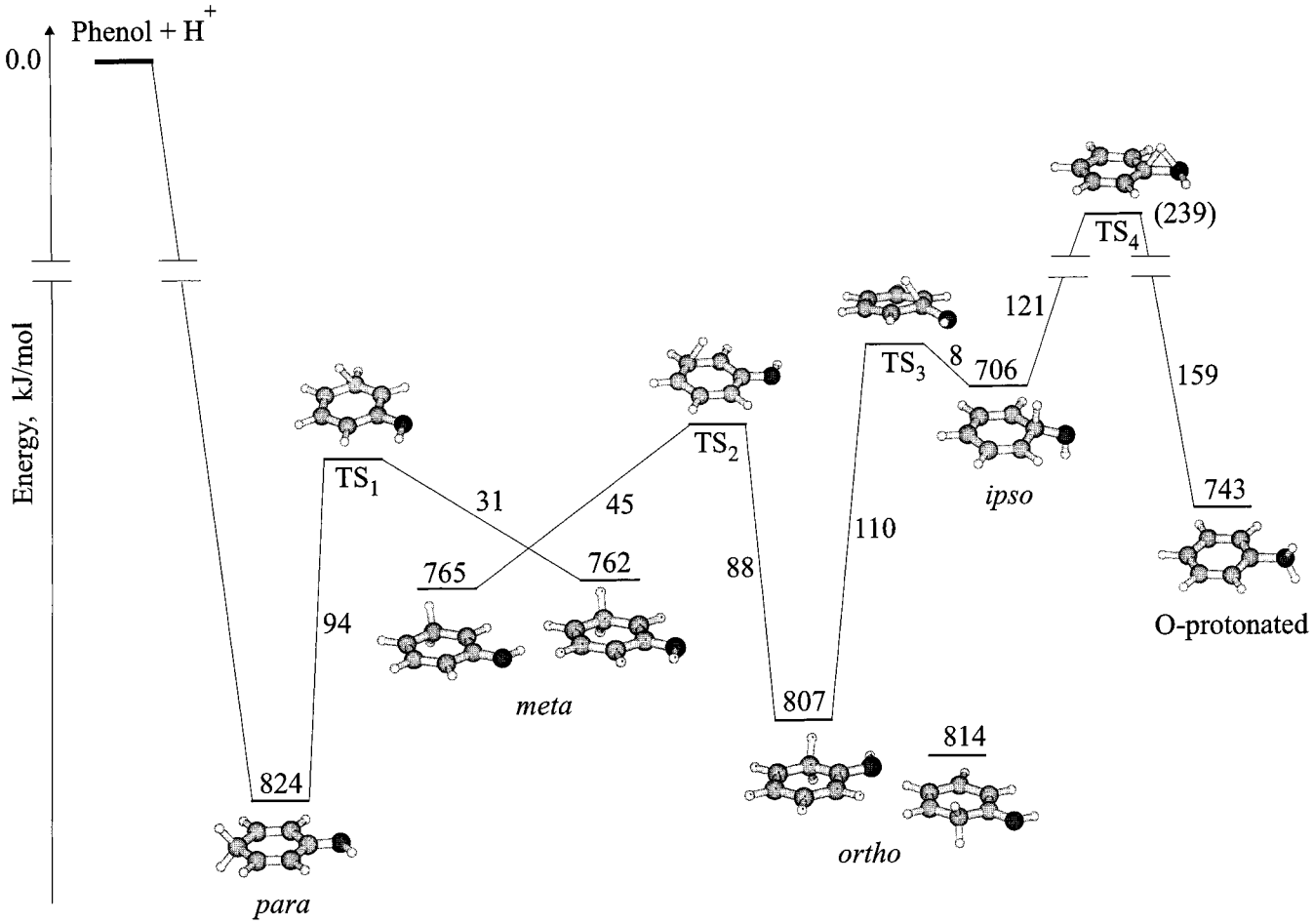

Figure 1. Portion of the potential energy surface of the protonated phenol showing the excess proton migration between the adjacent heavy atoms. Values in kJ/mol obtained from B3LYP/6-31+G(d,p) + ZPE computations.

ν_{OH} mode by 89 and 93 cm^{-1}, and also the blue shifts of the τ_{OH} mode by 281 cm^{-1} and 277 cm^{-1}, respectively. This implies a participation of the lone pairs of oxygen in stabilizing the arenium ion that leads to increasing the PA of the phenyl moiety. The meta-protonation shifts the corresponding vibrations by only 30 cm^{-1} and 69 cm^{-1} compared to those in the neutral molecule. A similarity in the frequency shifts of the ν_{OH} and τ_{OH} modes in both para- and ortho-protonated structures and their energies suggests that the regioselectivity of the protonation of phenol is mainly governed by resonance factors.

B. Proton Affinities of Halophenols. In Table 3 we collect the PA's of a series of monohalogenated phenols obtained at the B3LYP/6-31+G(d,p) + ZPE level. The PA's for fluorophenols are found to be in a reasonable agreement with the recent ion cyclotron resonance data,[47] namely, 797 kJ/mol (exptl = 788 kJ/mol) for 2-fluorophenol, 813 kJ/mol (exptl = 802 kJ/mol) for 3-fluorophenol, and 787 (exptl = 776 kJ/mol) for 4-fluorophenol, and thus approach experimental the PA with a quasi systematic overestimation of ca. 10−12 kJ/mol. To our knowledge, no experimental PA's of Cl-, Br-, and I-substituted phenols have been available so far.

Let us first consider the 2- and 3-halophenols. As seen in Table 3, irrespective of the nature of X atom, the para position remains the most attractive protonation site, followed by two ortho positions, C_6 and C_2, respectively. All structures protonated at these sites lie within 20 kJ/mol above the corresponding global C_4 minima (Table 3). The other sites are less accessible for protonation. As envisaged by the classical resonance model, the lower energy protonated structures always have the OH and X groups in the para and ortho positions relative to the protonation site. Among them, the structures where the OH group is attached in para and the X atom is attached in ortho reach the global minimum on the PES of a given X-substituted protonated phenol, featuring the highest PA's in the whole series, viz., 813 kJ/mol in 3-fluorophenol, 815 kJ/mol in 3-chlorophenol, 818

TABLE 3: B3LYP/6-31+G(d,p) Proton Affinities (kJ/mol) of Halogenated Phenols[a]

protonation site	C_1	C_2	C_3	C_4	C_5	C_6	O
substitution							
2-F	711	749	764	**797**	761	784	731
3-F	672	802	683	**813**	732	804	721
4-F	709	**787**	753	756	−	−	729
2-Cl	700	756	757	**801**	760	790	715
3-Cl	679	798	699	**815**	735	811	724
4-Cl	709	**789**	756	771	−	−	727
2-Br	702	763	760	**806**	763	795	736
3-Br	683	801	716	**818**	738	815	727
4-Br	713	**792**	759	784	−	−	728
2-I	710	791	767	**813**	769	803	743
3-I	691	807	−	**823**	746	820	730
4-I	719	791	765	**816**	−	−	731

[a] Atoms numbering is shown in Scheme 1. In *meta*-fluorophenols, the OH bond leans away from the substituent; in all other meta-substituted phenols, toward it, providing the most stable neutral structures. In the case of *para*-X-phenols, two pairs of structures with the protonation sites on C_2-C_6 and C_3-C_5 atoms, respectively, are energetically close. Notice that the present optimization procedure started initially from *meta*-iodophenol protonated at the same position, converged to the lower energy structure with both I and excess H^+ residing on the para site.

TABLE 4: Frequencies (cm^{-1}) of the OH Torsional and Stretching Vibrations in the Protonated vs Unprotonated Fluorophenols

Structure	τ_{OH}	ν_{OH}	Structure	τ_{OH}	ν_{OH}	Structure	τ_{OH}	ν_{OH}
	411	3802		330	3831		304	3833
	399	3780		613	3738		306	3809
	684	3686		594	3747		621	3735
	370	3780		400	3798			
	655	3692		561	3755			

kJ/mol in 3-bromophenol, and 823 kJ/mol in 3-iodophenol. Such behavior can be accounted for by a better conjugation of the oxygen's lone pair with the ring compared to that of the X groups. The 3-X-phenols (X = Cl, Br, and I) protonated at the C_4 and C_6 positions are nearly isoenergetic; their PA's are equal to 815 and 811 kJ/mol in 3-chlorophenol, 818 and 815 kJ/mol in 3-bromophenol, and 823 and 820 kJ/mol in 3-iodophenol, whereas the C_2-protonated species lie slightly higher in energy due to a steric repulsion with the OH group.

In para-halogenated phenols (X = F, Cl, and Br), the excess proton prefers to reside in ortho positions. On the contrary, in *para*-iodophenol, the protonated structure with both I and the excess H^+ residing in the para site, has the lowest energy.

In Table 4 we present the characteristic frequencies of the torsional τ_{OH} and stretching ν_{OH} vibrational modes in the neutral and protonated fluorophenols. The τ_{OH} vibration is directly related to distortions in π-electronic system which was experimentally demonstrated for a wide variety of substituted phenols.[48] It was particularly shown that the π-electron donor substituents at the para position lower the τ_{OH} frequency compared to the unsubstituted phenol, while the π-electron acceptor ones act in the opposite way. The present calculations concur with such findings. In neutral fluorophenols, the τ_{OH} mode is centered at 304 cm^{-1} (cf. 330 cm^{-1} in the unsubstituted phenol) (280 cm^{-1})[48b] for *para*-fluorophenol, 330 cm^{-1} (318.5 cm^{-1})[48b] for *meta*-fluorophenol, and is blue-shifted to 411 cm^{-1} (379 cm^{-1})[48c] for *ortho*-fluorophenol due to the hydrogen bonding (see Table 4). In systems without the hydrogen bonding, the τ_{OH} frequency is blue-shifted upon protonation depending on the protonation site. In para- and ortho-protonated phenols which are resonance-stabilized via the structures with the doubly bonded oxygen atom and demonstrate the highest PA, these shifts are very pronounced and comprise of 317 cm^{-1} in the C_6-protonated *para*-fluorophenol, 283 cm^{-1} in C_2-protonated, 264 cm^{-1} in C_4-protonated, and 231 cm^{-1} in C_6-protonated *meta*-fluorophenols. In meta-protonated structures, a blue shift of the τ_{OH} becomes smaller, viz., 2 cm^{-1} in *para*-fluorophenol, and 70 cm^{-1} in *meta*-fluorophenol. In *ortho*-fluorophenols, the effect of the protonation site on τ_{OH} is less evident due to its interplay with the effects of hydrogen bonding. The ν_{OH} frequency behaves in a similar manner with respect to protonation site, although shifts are opposite, as in the parent phenol molecule. By analogy with the torsional frequency, it reveals the maximum shifts in para- and ortho-protonated structures, viz., 98 cm^{-1} in C_6-protonated *para*-fluorophenol, 93 cm^{-1} in C_2-protonated, 84 cm^{-1} in C_4-protonated, and 76 cm^{-1} in C_6-protonated *meta*-fluorophenols. In the hydrogen-bonded systems, both the hydrogen bonding and distortions in π-electronic system caused by protonation behave coherently with respect to the ν_{OH} frequency toward a weakening of the OH bond and thus moving ν_{OH} to lower frequencies. The predicted red shifts of the ν_{OH} mode in these systems become even more pronounced: 116 cm^{-1} in C_4-protonated and 110 cm^{-1} in C_6-protonated 2-fluorophenols.

Closing this section, we would like to make some additional remarks on the protonation at the X atoms. In the case of 3-X-phenols, these structures occupy local minima on the corresponding PES lying, however, consistently above the high energy ipso-protonated phenols, except for 3-iodophenol in which an ipso protonation is less favorable by 13 kJ/mol than an I-protonation. The calculated PA's for the X-protonated 3-halophenols are the following: 613 kJ/mol for 3-fluorophenol, 676 kJ/mol for 3-chlorophenol, 680 kJ/mol for 3-Br-phenol, and 704 kJ/mol for 3-iodophenol.

C. Proton Affinities of Anisole and Fluoroanisoles. Anisoles are phenol derivatives in which the hydroxyl OH group is replaced by the methoxy OCH_3 one. We examine only the ring-protonated structures of fluoroanisoles and the combinations showing the highest PA for the parent phenol. As expected, anisole reveals the same protonation pattern as phenol, although all of its local PA's appear to be larger, namely: 845 kJ/mol in para-(C_4)-protonation, 836 kJ/mol in ortho-(C_6)-protonation, and 780 kJ/mol in meta-(C_3)-protonation. Interestingly, we observe a similar correlation between the local PA's and the C−O bond shortening (Δr) and the blue-shifting ($\Delta\nu_{CO}$) of the fundamental mode with the dominant contribution of ν_{CO} vibration. These Δr and $\Delta\nu_{CO}$ take the following values: 0.03 Å and 28 cm^{-1} in C_3-protonated anisole, 0.07 Å and 103 cm^{-1} in C_4-protonated anisole, 0.03 Å and 29 cm^{-1} in C_5-protonated anisole, and finally, 0.07 Å and 81 cm^{-1} in C_6-protonated anisole. The PA's of fluoroanisoles are equal to 820 kJ/mol (exptl = 807)[47] for 2-fluoroanisole, 835 kJ/mol (exptl = 826)[47] for 3-fluoroanisole, and 809 kJ/mol (exptl = 796)[47] for 4-fluoroanisole. An average overestimation of ca. 12 kJ/mol by the B3LYP/6-31+G(d,p) can again be noticed.

D. Correlation between Protonation Sites and Local Reactivity Indices. Having established the preferential sites of protonation in X-phenols, we now attempt to correlate them with the DFT-based reactivity indices whose definitions[49] and evaluations[50−52] are well established. The condensed Fukui functions (f)[51] on an atom, say k, in a molecule with N electrons are defined as

$$f_k^+ = [q_k(N+1) - q_k(N)] \qquad \text{for nucleophilic attack}$$

and

$$f_k^- = [q_k(N) - q_k(N-1)] \qquad \text{for electrophilic attack}$$

where q_k is the electronic population of atom k in the molecule under consideration. The local softness parameter can be then defined as follows:

$$s_k^{\,i} = f_k^{\,i} S \quad \text{where i} = + \text{ or } -$$

Within the finite difference approximation, the global softness, S, can be approximated by

$$S = 1/(\text{IE} - \text{EA})$$

where IE and EA are the first vertical ionization energy and electron affinity of the molecule, respectively. As mentioned

TABLE 5: Calculated Fukui Functions and Local Softnesses of Phenol Using the B3LYP Method with Two Basis Sets

property	B3LYP/cc-pVDZ		B3LYP/cc-pVTZ	
vert-IE (eV)	8.30		8.45	
vert-EA (eV)	−1.92		−1.66	
S (au)	2.66		2.69	
s_k^+ (f_k^+)				
C_1	0.10	(0.04)[a]	0.04	(0.02)
C_2	0.33	(0.12)	0.39	(0.14)
C_3	0.27	(0.10)	0.25	(0.09)
C_4	0.23	(0.09)	0.31	(0.12)
O	0.09	(0.03)	0.12	(0.05)
s_k^-(f_k^-)				
C_1	0.18	(0.07)	0.08	(0.03)
C_2	0.30	(0.11)	0.36	(0.13)
C_3	−0.03	(−0.01)	−0.04	(−0.02)
C_4	0.78	(0.29)	0.83	(0.31)
O	0.42	(0.16)	0.48	(0.18)
ratio s_k^-/s_k^+				
C_1	1.79		1.94	
C_2	0.92		0.92	
C_3	−0.11		−0.17	
C_4	3.41		2.64	
O	4.59		3.91	

[a] The f_k values are in parentheses.

in the 'Computational Methods' section, all calculations are carried out through DFT procedures with B3LYP hybrid functional and two correlation consistent cc-pVDZ and cc-pVTZ basis sets. The electronic energies and gross atomic charges (q) for the $N + 1$ and $N - 1$ electron systems are calculated at the optimized geometry of the N-electron system due to the constraint of constant external potential in the definition of Fukui functions.[49] The electronic populations of various atoms were calculated according to the electrostatic potential-derived charges (keyword MK in Gaussian 98[35]) that are less method-dependent than the Mulliken population analyses.[53]

Let us first examine the situation of the parent phenol for which the local indices are summarized in Table 5. The results obtained with two basis sets of different quality are quite consistent with each other. The values for the C_5 and C_6 atoms are also close to those for C_3 and C_2, respectively, and thus omitted for the sake of simplification. In the present case, the *local softnesses for electrophilic attack* s^- is to be used to probe the protonation mechanism, that is, the larger the local softness, the stronger the basic site. It is clear that the C_4 carbon atom bears the largest softeness ($s^- = 0.83$), a value much larger than that of oxygen ($s^- = 0.48$). While the C_2 carbon has a significant softness ($s^- = 0.36$), the C_1 and C_3 atoms do not show much affinity for electrophiles. These observations are in accord with the proton affinities discussed above which unambiguously indicate the preferential protonation at the C_4 carbon of phenol, followed by that at C_2 carbon and oxygen.

In their recent study on protonation of aniline ($C_6H_5-NH_2$), Roy et al.[20] suggested that the ratio s_k^-/s_k^+, termed as "relative nucleophilicity" and a measure of "local polarizability", should be considered as they produce more reliable results as a reactivity descriptor than the local softness s_k^-. Examination of the results listed in Table A which also lists the s_k^+ values and the quantities s_k^-/s_k^+ shows that *the ratio does not hold true for phenol protonation*. In fact the oxygen atom bears the largest ratio followed by the C_4. Among the ring carbon atoms, while the C_4 has the largest ratio (which is correct), the C_1 has a larger ratio than the C_2 one, which is not correct.

Tables 6 and 7 list the local softnesses and Fukui functions of the fluoro- and chlorosubstituted phenols, respectively. The values of s_k^- suggest the following protonation ordering:

(a) fluorophenols:

2-F, O > C_4 > C_6; 3-F, C_4 > C_6 > O, and

4-F, O > C_4 > C_6 > C_2

(b) chlorophenols:

2-Cl, C_4 > O > C_6; 3-Cl, C_4 > C_6 > O, and

4-Cl, O > C_6 > C_2

TABLE 6: Local Indices in Fluorophenols Obtained from B3LYP/cc-pVTZ Calculations

property	2-F-phenol		3-F-phenol		4-F-phenol	
vert-IE (eV)	8.63		8.65		8.46	
vert-EA (eV)	−1.54		−1.52		−1.30	
S (au)	2.677		2.676		2.790	
s_k^+ (f_k^+)						
C_1	0.18	(0.07)[a]	−0.20	(−0.08)	0.08	(0.03)
C_2	0.07	(0.02)	0.70	(0.26)	0.36	(0.13)
C_3	0.44	(0.17)	−0.06	(−0.22)	0.37	(0.14)
C_4	0.22	(0.08)	0.40	(0.15)	0.14	(0.05)
C_5	0.24	(0.09)	0.32	(0.12)	0.38	(0.14)
C_6	0.32	(0.12)	0.54	(0.20)	0.45	(0.16)
O	0.18	(0.07)	0.23	(0.09)	0.12	(0.04)
s_k^-(f_k^-)						
C_1	0.19	(0.07)	−0.03	(−0.01)	0.20	(0.07)
C_2	0.25	(0.09)	0.29	(0.11)	0.24	(0.09)
C_3	−0.05		−0.10	(−0.04)	0.23	(0.08)
C_4	0.75	(0.28)	0.92	(0.34)	0.33	(0.12)
C_5	0.10	(0.04)	−0.25	(−0.09)	0.20	(0.07)
C_6	0.56	(0.21)	0.74	(0.28)	0.31	(0.11)
O	1.32	(0.50)	0.43	(0.16)	0.46	(0.17)
ratio s_k^-/s_k^+						
C_1	1.01		0.12		2.57	
C_2	3.83		0.42		0.68	
C_3	−0.11		1.62		0.62	
C_4	3.44		2.32		2.58	
C_5	0.41		−0.77		0.51	
C_6	1.75		1.38		0.70	
O	7.42		1.90		3.83	

[a] The f_k values are in parentheses.

TABLE 7: Local Indices in Chlorophenols Obtained from B3LYP/cc-pVTZ Calculations

property	2-Cl-phenol		3-Cl-phenol		4-Cl-phenol	
vert-IE (eV)	8.55		8.56		8.34	
vert-EA (eV)	−1.30		−1.28		−1.25	
S (au)	2.760		2.764		2.838	
s_k^+ (f_k^+)						
C1	0.39	(0.14)[a]	−0.18	(−0.07)	0.06	(0.02)
C2	−0.46	(−0.17)	0.89	(0.32)	0.37	(0.13)
C3	0.75	(0.27)	−0.63	(−0.23)	0.48	(0.17)
C4	0.06	(0.02)	0.69	(0.25)	0.35	(0.12)
C5	0.47	(0.17)	0.09	(0.03)	0.45	(0.16)
C6	0.15	(0.05)	0.55	(0.20)	0.49	(0.17)
O	0.17	(0.60)	0.21	(0.08)	0.11	(0.04)
s_k^- (f_k^-)						
C1	0.25	(0.09)	−0.02	(−0.01)	0.12	(0.04)
C2	−0.04	(−0.02)	0.34	(0.12)	0.28	(0.10)
C3	0.04	(0.01)	−0.40	(−0.14)	0.27	(0.10)
C4	0.71	(0.26)	0.98	(0.36)	−0.53	(−0.19)
C5	0.17	(0.06)	−0.24	(−0.09)	0.25	(0.09)
C6	0.15	(0.05)	0.71	(0.26)	0.35	(0.12)
O	0.49	(0.18)	0.40	(0.14)	0.42	(0.15)
ratio s_k^-/s_k^+						
C1	0.65		0.10		2.14	
C2	0.09		0.37		0.77	
C3	0.05		0.63		0.57	
C4	11.82		1.42		−1.52	
C5	0.35		−2.66		0.55	
C6	1.00		1.29		0.71	
O	2.94		1.90		3.84	

[a] The f_k values are in parentheses.

In comparison with the calculated PA mentioned in preceding sections, a few points are worth noting:

(i) it seems not sensible to compare the local softnesses of atoms having different atomic numbers, for example, the one of a carbon with that of an oxygen. In other words, similar to the shortcomings of net atomic charges or electrostatic potentials,[54] this local descriptor seems not to be able to differentiate the relative basicities of heteroatoms. Russo et al.[21] have also drawn a similar conclusion from their analysis of the *orbital local softnesses*.

(ii) The local softness behaves more regularly among the ring carbon atoms. In fact, for both 2-X and 3-X phenols, the local softness points toward a para protonation in agreement with explicit computations of PA's. While for 4-Cl the local softness correctly predicts the preference of C_6 and C_2, the situation is more confusing in 4-F where the s^- values of all carbons are similar to each other, with a marginally larger value for C_4 followed by C_6 and C_2 (if oxygen omitted).

(iii) In all cases, the ratio s_k^-/s_k^+ is not able to unravel the preferable protonation site.

(iv) There is no correlation between the absolute values of local softnesses with the PA's at the ring carbon centers.

These drawbacks raise the question as to whether it is meaningful to use the local softness in distinguishing the protonation of atoms of different nature. Similar to the case of two heteroatoms, such as O and C, when a X-substituent strongly modifies the electronic environment of the carbon, a perturbation type of treatment could also no longer be applied to the C(H) and C(X) centers.

Although the local softness includes, by definition, both the differences of frontier orbitals of the neutral substrate and the differential electron densities between the neutral and ionized states, as expressed in the global softness and Fukui functions, the actual computations of these quantities suffer from some severe limitations. In practice, as mentioned above, the approximation of electron densities boils down to the evaluation of the atomic net charges. It is well-known that the latter terms are method-dependent and their computations could show some erratic behaviors. After all, the proton is a very strong electrophile (and very hard) and its approach polarizes the whole medium due to its small size and basically modifies the molecular and electronic structure, and the softness of the substrate. Because the DFT-based indices are defined at constant chemical potentials, it is obvious that they are not sensitive enough to foresee the situation with drastic changes following protonation.

4. Concluding Remarks

In the present theoretical study, we have addressed the problem of determining the preferable protonation sites in phenol and halogenated phenols in the gas phase by calculating their local proton affinities and also the DFT-based local reactivity descriptors from the neutral molecules.

Comparing with available experimental data, the B3LYP/6-31+G(d,p) level overestimates the PA's of halophenols by about 10 kJ/mol. Because this overestimation is quite systematic, a simple empirical correction of the same amount could be applied to the B3LYP values in order to obtain realistic proton affinities.

The ring carbon atom in the para position with respect to the OH group (C_4) is by far the most preferable protonation site, either in the parent phenol or in the ortho (C_2 or C_6) and meta (C_3 or C_5) halogen-substituted derivatives. Regarding the *para*-X-phenols, while fluorine, chlorine, and bromine modify the pattern in a favor of the ortho protonation, iodine upholds the para protonation. The same sequence of protonation also holds for fluoroanisoles.

For a parent protonated phenol, the portion of the PES showing the migration of the excess proton between the protonation sites has been discussed.

A correlation between the local PA's and the red and blue shifts in the ν_{OH} and τ_{OH} vibrational modes, respectively, indicates that a regioselectivity of the protonation in the phenol ring is mainly controlled by the resonance factors.

Overall, it seems that the condensed Fukui function (f_k^-) or the related local softness (s_k^-), as computed throughout the employed approximation, could cautiously be used as a descriptor for ring protonation of phenol derivatives. The ratio s_k^-/s_k^+ recently advocated as a protonation descriptor, does not perform well in this case. Much more caution also needs to be exercised when comparing the local descriptors of atoms having different nature.

Note Added in Proof. A recent paper[55] reported the IR spectra of the protonated phenol complexes with one and two argon ligands. The IR results revealed the presence of two different protonated forms at oxygen and at the ring. This is in agreement with our results shown in Figure 1: if formed, the O-protonated phenol could resist to unimolecular rearrangements whereas the migration of the proton within the phenyl ring (*ortho*, *meta* and *para* positions) is a more facile process. Therefore it is more difficult to observe the *meta*-protonated phenols, even though it is more stable than the O-protonated isomer.

Acknowledgment. The authors are grateful to the GOA program (O.T. and N.N.P.T.), KU-Leuven Research Council (E.S.K.), and FWO-Vlaanderen (M.T.N.) for financial support. We aslo thank Dr. Asit Chandra at Tsukuba, Japan, for stimulating discussion.

References and Notes

(1) Bell, R. P. *The Proton in Chemistry*; Cornell University Press: Ithaca, New York, 1959; p 20.

(2) Ng, C. Y.; Trevor, D. J.; Tiedemann, P. W.; Ceyer, S. T.; Kroebusch, P. L.; Mahan, B. H.; Lee, Y. T. *J. Chem. Phys.* **1977**, *67*, 4235.

(3) Peterson, K. A.; Xantheas, S. S.; Dixon, D. A.; Dunning, T. H., Jr. *J. Phys. Chem. A* **1998**, *102*, 2449.

(4) Kuck, D. *Angew. Chem. Int. Ed*. **2000**, *39*, 125.

(5) Pl'iva, J.; Johns, J. W. C.; Goodman, L. *J. Mol. Spectrosc*. **1991**, *148*, 427.

(6) (a) Chong, S. L.; Franklin, J. L. *J. Am. Chem. Soc.* **1972**, *94*, 6630. (b) Aue, D. H.; Bowers, M. T. In *Gas-Phase Ion Chemistry*; Bowers, M. T., Ed.; Academic Press: New York, 1979; Vol. 2, p 1.

(7) Kryachko, E. S.; Nguyen, M. T. *J. Phys. Chem. A* **2001**, *105*, 153.

(8) McIver, R. T., Jr.; Dunbar, R. C. *Int. J. Mass Spectrom. Ion Phys.* **1971**, *7*, 471.

(9) Lau, Y.; Kebarle, P. *J. Am. Chem. Soc.* **1976**, *98*, 7452.

(10) Hunter, E. P.; Lias, S. G. *J. Phys. Chem. Ref. Data* **1998**, *27*, 413.

(11) DeFrees, D. J.; McIver, R. T., Jr.; Hehre, W. J. *J. Am. Chem. Soc.* **1977**, *99*, 3853.

(12) Eckert-Maksic, M.; Klessinger, K.; Maksic, Z. B. *Chem. Phys. Lett.* **1995**, *232*, 472.

(13) Bagno, A.; Scorrano, G. *J. Phys. Chem.* **1996**, *100*, 1536 and references therein.

(14) Bader, R. F. W.; Chang, C. *J. Phys. Chem.* **1989**, *93*, 5095 and references therein.

(15) Kovacek, D.; Maksic, Z. B.; Novak, I. *J. Phys. Chem. A* **1997**, *101*, 1147.

(16) Raos, G.; Gerratt, J.; Karadakov, P. B.; Cooper, D. L.; Raimondi, M. *J. Chem. Soc., Faraday Trans.* **1995**, *91*, 4011.

(17) Nguyen, M. T.; Hegarty, A. F.; Ha, T. K.; De Mare, G. R. *J. Chem. Soc., Perkin Trans*. 2 **1986**, 147.

(18) (a) Sanderson, R. T. *Polar Covalence*; Academic Press: New York, 1983. (b) Baeten, A.; De Proft, F.; Geerlings, P. *Int. J. Quantum Chem.* **1996**, *60*, 931.

(19) (a) Marino, T.; Russo, N.; Tocci, E.; Toscano, *J. Mass Spectrom.* **2001**, *36*, 301. (b) Marino, T.; Russo, N.; Silicia, E.; Toscano, M.; Mineva, T. *Adv. Quantum Chem.* **2000**, *36*, 93. (c) Russo, N.; Toscano, M.; Grand, A.; Jolibois, F. *J. Comput. Chem.* **1998**, 19, 989. (d) Topol, I. A.; Burt, S. K.; Russo, N.; Toscano, M. *Theochem.* **1998**, *430*, 41; *J. Am. Soc. Mass Spectrom.* **1999**, *10*, 318.

(20) Roy, R. K.; De Proft, F.; Geerlings, P. *J. Phys. Chem. A* **1998**, *102*, 7035.

(21) Russo, N.; Toscano, T.; Grand, A.; Mineva, T. *J. Phys. Chem. A* **2000**, *104*, 4017.

(22) Chandra, A. K.; Nguyen, M. T. *J. Chem. Soc., Perkin Trans. 2* **1997**, 1415.

(23) Raspoet, G.; Nguyen, M. T.; Kelly, S.; Hegarty, A. F. *J. Org. Chem.* **1998**, *63*, 9669.

(24) Nguyen, M. T.; Raspoet, G.; Vanquickenborne, L. G. *J. Phys. Org. Chem.* **2000**, *13*, 46.

(25) Nguyen, M. T.; Raspoet, G. *Can. J. Chem.* **1999**, *77*, 817.

(26) Chandra, A. K.; Geerlings, P.; Nguyen, M. T. *J. Org. Chem.* **1997**, *62*, 6417.

(27) Nguyen, L. T.; Le, N. T.; De Proft, F.; Chandra, A. K.; Langenaeker, W.; Nguyen, M. T.; Geerlings, P. *J. Am. Chem. Soc.* **1999**, *121*, 5992.

(28) Sengupta, D.; Chandra, A. K.; Nguyen, M. T. *J. Org. Chem*. **1997**, *62*, 6404.

(29) Chandra, A. K.; Nguyen, M. T. *J. Comput. Chem*. **1998**, *19*, 195.

(30) Chandra, A. K.; Nguyen, M. T. *J. Phys. Chem. A* **1998**, *102*, 6181.

(31) Le, T. N.; Nguyen, L. T.; Chandra, A. K.; De Proft, F.; Nguyen, M. T.; Geerlings, P. *J. Chem. Soc., Perkin Trans 2* **1999**, 1249.

(32) Chandra, A. K.; Michalak, A.; Nguyen, M. T.; Nalewajski, R. *J. Phys. Chem. A* **1998**, *102*, 10188.

(33) Chandra, A. K.; Uchimaru, T.; Nguyen, M. T. *J. Chem. Soc., Perkin Trans. 2* **1999**, 2117.

(34) Nguyen, M. T.; Chandra, A. K.; Sakai, S.; Morokuma, K. *J. Org. Chem.* **1999**, *64*, 65.

(35) Frisch, M. J.; Trucks, G. W.; Schlegel, H. B.; Scuseria, G. E.; Robb, M. A.; Cheeseman, J. R.; Zakrzewski, V. G.; Montgomery, J. A., Jr.; Stratmann, R. E.; Burant, J. C.; Dapprich, S.; Millam, J. M.; Daniels, A. D.; Kudin, K. N.; Strain, M. C.; Farkas, O.; Tomasi, J.; Barone, V.; Cossi, M.; Cammi, R.; Mennucci, B.; Pomelli, C.; Adamo, C.; Clifford, S.; Ochterski, J.; Petersson, G. A.; Ayala, P. Y.; Cui, Q.; Morokuma, K.; Malick, D. K.; Rabuck, A. D.; Raghavachari, K.; Foresman, J. B.; Cioslowski, J.; Ortiz, J. V.; Stefanov, B. B.; Liu, G.; Liashenko, A.; Piskorz, P.; Komaromi, I.; Gomperts, R.; Martin, R. L.; Fox, D. J.; Keith, T.; Al-Laham, M. A.; Peng, C. Y.; Nanayakkara, A.; Gonzalez, C.; Challacombe, M.; Gill, P. M. W.; Johnson, B. G.; Chen, W.; Wong, M. W.; Andres, J. L.; Head-Gordon, M.; Replogle, E. S.; Pople, J. A. *Gaussian 98*, revision A.9; Gaussian, Inc.: Pittsburgh, PA, 1998.

(36) (a) Lee, C.; Yang, W.; Parr, R. G. *Phys. Rev. B* **1988**, *37*, 785. (b) Becke, A. D. *J. Chem. Phys*. **1993**, *98*, 5648.

(37) (a) Schwerdtfeger, P.; Dolg, M.; Schwarz, W. H.; Bowmaker, Boyd, P. D. W. *J. Chem.* Phys. **1989**, *91*, 1672. (b) Bergner, A.; Dolg, M.; Kuchle, W.; Stoll, H.; Preuss, H. *Mol. Phys*. **1993**, *80*, 1431. (c) Basis sets were obtained from the Extensible Computational Chemistry Environment Basi Set Database, as developed and distributed by the Molecular Science Computing Facility, Environmental and Molecular Sciences, Pacific Laboratory, P.O Box 999, Richland, Washington, 99352, U.S.; http://www.emsl.pnl.gov: 2080/forms/basisform.html.

(38) Pedersen, T.; Larsen, N. W.; Nygaard, L. *J. Mol. Struct*. **1969**, *4*, 59.

(39) Bist, H. D.; Brand, J. C. D.; Williams, D. R. *J. Mol. Spectrosc*. **1967**, *24*, 402.

(40) (a) Keresztury, G.; Billes, F.; Kubinyi, M.; Sundius, T. *J. Phys. Chem. A* 1**998**, *102*, 1371. (b) Roth, R.; Imhof, P.; Gerhards, M.; Schumm, S.; Kleinermanns, K. *Chem. Phys*. **2000**, *252*, 247.

(41) Varsányi, G. *Assignments for Vibrational Spectra of 700 Benzene Derivatives*; John Wiley: New York, 1974.

(42) Raghavachari, K.; Trucks, G. W.; Pople, J.A.; Head-Gordon, M. *Chem. Phys. Lett.* **1989**, *157*, 479.

(43) (a) De Proft, F.; Martin, J. M. L.; Geerlings, P. *Chem. Phys. Lett.* **1996**, *256*, 400. (b) Chermette, H. *J. Comput. Chem.* **1999**, *20*, 129 and references therein. (c) Silicia, E.; Russo, N.; Mineva, T. *J. Phys. Chem. A* **2001**, *105*, 442 and references therein. (d) Mineva, T.; Russo, N.; Silicia, E. *J. Am. Chem. Soc.* **1998**, *120*, 9093. (e) Toro-Labbe, A. *J. Phys. Chem. A* **1999**, *103*, 4398. (f) De Proft, F.; Langenaker, W.; Geerlings, P. *J. Phys. Chem.* **1993**, *97*, 1826. (g) Balewander, R.; Komorowski, L. *J. Chem. Phys.* **1998**, *109*, 5203 and references therein. (h) Roy, R. K.; Pal, S.; Hirao, K. *J. Chem. Phys.* **1999**, *110*, 9236.; *J. Chem. Phys.* **2000**, *113*, 1372. (i) Uchimaru, T.; Chandra, A. K.; Kawahara, S.-I.; Matsumura, K.; Tsuzuki, S.; Mikami, M. *J. Phys. Chem. A* **2001**, *105*, 1343.

(44) (a) Gadosy, T. A.; McClelland, R. A. *J. Mol. Struct.* **1996**, *396*, 1. (b) E. Clar, Die Chemie, **1943**, *56*, 293. (c) Pullman, B.; Pullman, A. *Quantum Biochemistry*; Wiley-Interscience: New York, 1963, p 122.

(45) (a) Nyquist, R. H. *Spectrochim. Acta* **1963**, *19*, 1655. (b) Campagnaro, G. E.; Wood, J. L. *J. Mol. Struct.* **1970**, *6*, 117.

(46) Larsen, N. W.; Nicolaisen, F. M. *J. Mol. Struct*. **1974**, *2*, 29.

(47) Bogdanov, B.; van Duijn, D.; Ingemann, S. *Proceedings of the XXth Congress on Mass Spectrometry*, Madrid, Spain, July 2000.

(48) (a) Fateley, W. G.; Carlson, G. L.; Bentley, F. F. *J. Phys. Chem*. **1975**, *79*, 199. (b) Fateley, W. G.; Miller, F. A.; Witkowski, R. E. Technical Documentary Report No. AFML-TR-66-408; Air Force Materials Laboratory/LPH: Wright-Patterson Air Force Base, Ohio, Jan 1967. (c) Carlson, G. R.; Fateley, W. G.; Manocha, A. S.; Bentley, F. F. *J. Phys. Chem*. **1972**, *76*, 1553.

(49) Parr, R. G.; Yang, W. *J. Am. Chem. Soc.* **1984**, *106*, 4049.

(50) Geerlings, P.; De Proft, F.; Langenaeker, W. *Adv. Quantum Chem.* **1999**, *33*, 301.
(51) Mineva, T.; Neshev, N.; Russo, N.; Silicia, E.; Toscano, M. *Adv. Quantum Chem.* **1999**, *33*, 273.
(52) Yang, W.; Mortier, W. J. *J. Am. Chem. Soc.* **1986**, *108*, 5708.
(53) De Proft, F.; Martin, J. M. L.; Geerlings, P. *Chem. Phys. Lett.* **1996**, *250*, 393.
(54) Nguyen, M. T.; Ha, T. K. *J. Mol. Struct. (THEOCHEM)* **1982**, *82*, 355.
(55) Solcà, N.; Dopfer, O. *Chem. Phys. Lett.* **2001**, *342*, 191.